THE UNIVERSITY OF WARWICK

For more information, please contact the WRAP Team at: **warwickpublicationswrap**

highlight your research

http://go.warwick.ac.uk/lib-publications

1 **Pre-existing virus-specific CD8^{+} T-cells provide protection against**

2 **pneumovirus-induced disease in mice**

3

4 *Mary J. G. van Helden[a], Peter J. S. van Kooten[a], Cornelis P. J. Bekker[a], Andrea*

5 *Gröne[b], David J. Topham[c], Andrew J. Easton[c], Claire J. P. Boog[d], Dirk H. Busch[e],*

6 *Dietmar M. W. Zaiss[a], and Alice J. A. M. Sijts[a]*

7 *[a]Division of Immunology, Faculty of Veterinary Medicine, University of Utrecht,*

8 *Yalelaan 1, 3571 EK Utrecht, The Netherlands; [b]Division of Pathology, Faculty of*

9 *Veterinary Medicine, University of Utrecht, Yalelaan 1, 3571 EK Utrecht, The*

10 *Netherlands; [c]D. Smith Center for Vaccine Biology and Immunology, University of*

11 *Rochester Medical Center, 601 Elmwood Avenue, Rochester, NY 14642, USA;*

12 *[d]School of Life Sciences, Gibbet Hill Campus, University of Warwick, Coventry*

13 *CV4 7AL, UK; [e]Department of Vaccinology, Centre for Infectious Disease Control,*

14 *National Institute for Public Health and the Environment (RIVM), Antonie van*

15 *Leeuwenhoeklaan 9, 3721 MA Bilthoven, The Netherlands; [f]Institute for Medical*

16 *Microbiology, Immunology and Hygiene, Technische Universität München,*

17 *Trogerstrasse 30, 81675 München, Germany.*

18

19

20

21 *Correspondence to:* Dr. Alice J.A.M. Sijts or Dr. D. Zaiss, Division of Immunology,

22 Faculty of Veterinary Medicine, University of Utrecht, Yalelaan 1, 3584 CL Utrecht,

23 The Netherlands, Phone: +31302532471, Fax: +31302533555, e-mail:

24 e.j.a.m.sijts@uu.nl or d.zaiss@uu.nl

25

ABSTRACT

Pneumoviruses such as pneumonia virus of mice (PVM), bovine respiratory syncytial virus (bRSV) or human (h)RSV are closely related pneumoviruses that cause severe respiratory disease in their respective hosts. It is well-known that T-cell responses are essential in pneumovirus clearance, but pneumovirus-specific T-cell responses also are important mediators of severe immunopathology. In this study we determined whether memory – or pre-existing, transferred virus-specific CD8$^+$ T-cells provide protection against PVM-induced disease. We show that during infection with a sublethal dose of PVM, both natural killer (NK) cells and CD8$^+$ T-cells expand relatively late. Induction of CD8$^+$ T-cell memory against a single CD8$^+$ T- cell epitope, by dendritic cell (DC)-peptide immunization, leads to partial protection against PVM challenge and prevents Th2 differentiation of PVM-induced CD4 T-cells. In addition, adoptively transferred PVM-specific CD8$^+$ T-cells, covering the entire PVM-specific CD8$^+$ T-cell repertoire, provide partial protection from PVM-induced disease. From these data we infer that antigen-specific memory CD8$^+$ T-cells offer significant protection to PVM-induced disease. Thus, CD8$^+$ T-cells, despite being a major cause of PVM-associated pathology during primary infection, may offer promising targets of a protective pneumovirus vaccine.

Key words: Pneumoviruses; pneunomia virus of mice; NK cell; CD8$^+$ T-cell; vaccine

52 **Footnote**

53

54 *Abbreviations*: BAL, bronchoalveolar lavage; BALF, BAL fluid; DC, dendritic cell;

55 BM-DC, bone marrow derived DC; DCp, peptide-loaded DC; FI, formalin

56 inactivated; hRSV, human respiratory syncytial virus; ID, infectious dose; EID,

57 egg ID; i.n., intranasal; i.p., intraperitoneal; i.v., intravenous; MLN, mediastinal

58 lymph node; NK, natural killer; NS, nonstructural; p.i., post infection; pfu, plaque

59 forming units; PVM, pneunomia virus of mice; SEM, standard error of mean.

60

61

1. Introduction

Pneumoviruses are an important cause of respiratory infections in mammals [1]. One well-known member of the pneumovirus genus is hRSV, a major cause of severe respiratory disease in infants and elderly [2]. A failed vaccine trial using formalin-inactivated hRSV (FI-RSV) in the 1960s that led to enhanced disease instead of immune protection [3-6], has triggered intense efforts to elucidate how to induce immune responses that can prevent or protect against natural hRSV infection without causing pathology. Different studies in humans and mouse models have shown that antibodies can contribute to immune protection [7-10]. However, the antibodies induced during natural hRSV infection fail to prevent recurrent infections throughout life, indicating that also the efficacy of vaccine-induced neutralizing antibodies may be limited [7,11]. Controversy also exists concerning the precise role of the T cell compartment in pneumovirus-induced disease [12,13]. Several studies have shown that although T cells are essential in eradicating established infections [14], they also are important mediators of hRSV-induced immunopathology [15-19]. In murine models, especially Th2 skewing of the CD4$^+$ T-cell lineage after immunization with FI-RSV or hRSV-G protein encoding recombinant Vaccinia Virus vectors have been shown to lead to enhanced disease following subsequent hRSV infection [12,13,20]. Induction of CD8$^+$ T-cell responses, on the other hand, inhibited vaccine-enhanced pulmonary disease [21-23]. Thus, despite the notion that T cells play a role in pneumovirus-induced immunopathology, these studies suggest that vaccines designed to induce antipneumoviral CD8$^+$ T cell responses may offer an alternative to vaccines targeting the humoral response.

Pneumoviruses display a narrow host range and several species-specific variants have been described [1], adapted for evasion of defense mechanisms in

4

88   their specific hosts [24,25]. Therefore, instead of hRSV, its mouse-adapted variant

89   PVM is increasingly used to study pneumovirus-specific immune responses and

90   immunopathogenesis in mouse models. PVM and hRSV display a marked genetic

91   similarity and use similar evasion strategies [26-28]. Intranasal (*i.n.*) administration

92   of a low PVM inoculum results in effective replication and severe respiratory

93   disease in mice, with several hallmarks similar to severe hRSV disease in

94   humans, including severe pulmonary inflammation, edema, and influx of

95   granulocytes [29].

96   Although extensively studied during hRSV infections in mouse models,

97   only limited studies evaluated T cells in PVM infected mice [30,31]. Frey et al

98   showed that, like in hRSV-infection, T-cells are essential for viral elimination in

99   PVM-infected mice, but are also important mediators of infection-associated

100   pathology. This observation raises the question of whether a pneumovirus-vaccine

101   that targets CD8^{+} T cell responses would be safe. In this study, we used the PVM

102   mouse model of respiratory infection to determine whether pre-existing virus-

103   specific CD8^{+} T-cells may provide protection against pneumovius-induced

104   disease.

105

106

107

108   **2. Material and methods**

109   *2.1. Virus stocks, mice and infection*

110   PVM strain J3666 was passaged in mice to retain full pathogenicity and

111   hRSV strain A2 was grown in BSC-1 cells and concentrated as described [32]. For

112   both viruses, plaque assays on BSC-1 cells were performed to determine viral

113   titers. Influenza strains A/HK/x31 (H3N2) and A/PR/8/34 (H1N1) were grown as

114   described [33]. Age-matched 7-10 week old female BALB/c mice were purchased

115   from Charles River, anesthetized with isoflurane and then infected *i.n.* with $5x10^6$

116   pfu RSV in 50 μl, or with $1x10^5$ EID_{50} HKx31 or 150 EID_{50} PR8 in 30 μl PBS as

117   described [33], or with the indicated doses of PVM in 30 μl PBS. All animal

118   experiments were approved by the Committee on Animal Experiments of the

119   University of Utrecht.

120

121   *2.2. Sample preparation*

122   Mice were sacrificed by injection of sodium pentobarbital and

123   bronchoalveolar lavage (BAL) was collected by three times lavage with 1 ml PBS

124   containing 10 μM EDTA. Thereafter, lungs were perfused with PBS, excised,

125   minced and incubated in PBS containing collagenase (2.4 mg/ml; Roche Applied

126   Science) and DNase (1 mg/ml; Roche Applied Science) for 30 minutes at 37°C,

127   passed through a cell strainer and lymphocytes were purified using lympholyte-M

128   (Cederlane). For mRNA isolation, the right lung was placed in 1 ml TRIzol

129   (Invitrogen).

130

131   *2.3. Flow cytometry*

132   Fluorochrome-conjugated antibodies were purchased from eBioscience

133   [CD69 (H1.2F3), CD49b (DX5), TCRβ (H57-597), NKp46 (29A1.4), CD62L (MEL-

134   14), IFNγ (XMG1.2), CD8 (53-6.7), CD11c (N418), CD19 (MB19-1), CD4 (RM4-5),

135   MHC-II (m5/114.15.2)] or BD Pharmingen [Siglec-F (E50-2440)]. PE-labeled MHC

136   class I tetramers were prepared in collaboration with D. Busch (TU-Muenchen), by

137   refolding H2-K^d heavy chains and human β$_2$m in the presence of synthetic

138   influenza-derived NP$_{147-155}$ (TYQRTRALV), hRSV M2$_{82-90}$ (SYIGSINNI) or PVM

6

139   P$_{261-269}$ (CYLTDRARI). Cell surface markers were stained as described [34]. For

140   tetramer stainings, cells were incubated with 1 μg tetramer for 1 hour at 4 ^{0}C and

141   then stained for surface markers. To measure IFNγ production, BAL cells were

142   stimulated 1:1 with YAC cells for 4 hours (NK cell activation) or with 2 μM P$_{261-269}$

143   for 6 hours (CD8^{+} T-cell stimulation) in 100 μl RPMI medium containing 10% FCS,

144   glutamax, antibiotics and 30 μM β-mercaptoethanol, and 10 μM monensin and

145   then stained as described [34]. Cells were analyzed on a FACS Calibur or Canto II

146   (BD Biosciences) using FlowJo software (Tree Star).

147

148   *2.4. Preparation of peptide-loaded bone marrow (BM)-DC and FI-PVM*

149   Mouse BM-DC were expanded for 6 days in RPMI medium with 15% GM-

150   CSF (culture supernatant of X63Ag cells), activated overnight with 100 ng/ml LPS

151   and then pulsed for 1 hour with 2 μM P$_{261-269}$. Mice were immunized intravenously

152   (*i.v.*) with 5 x 10^{6} peptide-loaded BM-DC in 200 μl PBS. FI-PVM was prepared as

153   described [6] and was administered in 100 μl *s.c.* Mice were infected with PVM, 3-

154   5 weeks after immunization.

155

156   *2.5. Quantitative real-time PCR*

157   Total lung RNA was purified using TRIzol (Invitrogen) and cDNA was

158   transcribed (iScript cDNA Synthesis Kit; Bio-Rad Laboratories). PVM$_{SH}$ RT-PCR

159   was performed as described [35] in an iCycler (Bio-Rad Laboratories), 95 °C for

160   10 min and then 45 cycles of 95 °C for 15s and 60 °C for 60s. Copy numbers per

161   lung were calculated from a standard curve generated using serially diluted PVM-

162   SH cDNA. RT-PCR for IL-4, IFNγ and GAPDH were performed using the TaqMan

163   Gene Expression Assays (Applied Biosystems) Mm00445259, Mm00801778 and

164 Mm99999915. Relative expression of IL-4 and IFNγ normalized against GAPDH

165 were calculated using a fixed point of the standard curve as calibrator.

166

167 *2.6. Multiplex bead-based assay*

168   To quantify IL-4 and IFNγ, fluoresceinated microbeads coated with capture

169 antibodies (IL-4: BVD-1D11; IFN-γ:AN-18) were added to 50 μl BAL fluid and

170 incubated overnight at 4 °C. Cytokines were detected with biotinylated anti-IFNγ

171 (XMG1.2) and -IL-4 (BVD6-24G2), and PE-labeled streptavidin. Fluorescence was

172 measured using a Luminex model 100 XYP (Luminex, Austin, TX, USA).

173 Antibodies were purchased from BD Biosciences.

174

175 *2.7. Adoptive transfer of CD8⁺ T-cells*

176   Naïve and PVM-infected (d. 14 p.i.) donor mice were sacrificed, single cell

177 suspensions prepared of lungs, spleens and MLNs were mixed and stained with

178 PE-labeled antibodies against CD19, CD4, MHC-II and NKp46 (without Fc-block).

179 Negative selection was performed using a BD Influx (BD Biosciences). Recipient

180 mice received 5×10^6 enriched cells in 200 μl PBS *i.v.*, and then were infected

181 with PVM.

182

183 **3. Results**

184 *3.1. Dynamics of CD8⁺ T-cell responses in PVM-infected mice*

185 *I.n.* infection with 25 pfu of PVM strain J3666 induced severe but sublethal

186 disease in BALB/c mice, with weight reduction of approximately 15 - 20% of

187 original body weight (data not shown). During the first days of infection, PVM

188 rapidly replicated to high numbers (Fig. 1A). Viral copy numbers peaked at d. 8

189 p.i. and then declined.

190   In order to determine their protective capacity, we first studied CD8^{+} T-cell

191 kinetics during primary PVM infection and compared these with the well-described

192 CD8^{+} T- cell responses in influenza and hRSV-infected mice [36, 37]. The relative

193 proportions of CD8^{+} T-cells in the airways of PVM-infected mice strongly

194 increased over time (Fig. 1B), and from d. 10 onwards approximately 60% of

195 lymphocytes in the BAL were CD8^{+} T-cells. In influenza- and hRSV-infected mice,

196 initially, the proportions of CD8^{+} T-cells in the airways were higher than in PVM-

197 infected mice but then dropped, when relative proportions of CD8^{+} T-cells in PVM-

198 infected mice were still rising (Fig. 1B). Quantification of virus-specific CD8^{+} T-

199 cells with MHC class I tetramers containing a dominant epitope of either PVM

200 ($P_{261-269}$ [30]), influenza ($NP_{147-155}$ [38]) or hRSV ($M2_{82-90}$ [39]), demonstrated that

201 $NP_{147-155}$- and $M2_{82-90}$-specific CD8^{+} T-cells were detectable at d. 6 p.i. and

202 expanded until d. 8-10 p.i. when a plateau was reached (Fig. 1C). In PVM-infected

203 mice, the BAL did not contain any $P_{261-269}$-specific CD8^{+} T-cells at d. 6 p.i, and only

204 a small population of $P_{261-269}$-specific CD8^{+} T-cells could be detected at d. 8 p.i.

205 (Fig. 1D, E). The relative proportions of $P_{261-269}$ tetramer^{+} CD8^{+} T-cells further

206 increased until d. 10 p.i. after which levels remained high (Fig. 1D, E). To

207 determine whether PVM -specific CD8^{+} T-cell were functional, we quantified IFNγ

208 production in virus-specific CD8^{+} T-cells after *ex vivo* $P_{261-269}$ stimulation.

209 Consistent with earlier publications [30,37], we found that IFNγ producing $P_{261-269}$-

210 specific CD8^{+} T-cells were barely detectable at d. 8 of infection (Fig. 1F, G) but

211 then increased in numbers. At any time point of infection, the relative proportions

212 of IFNγ-producing $P_{261-269}$-specific CD8^{+} T-cells remained lower than that of $P_{261-269}$

213 tetramer-stained cells. From these data we conclude that high proportions of CD8^{+}

9

214   T-cells migrate to the lungs of PVM infected mice and that the appearance of

215   virus-specific CD8$^+$ T-cells in the airways is slightly delayed compared to influenza

216   virus- or hRSV-infected mice.

217

218   *3.2. Dynamics of innate responses to PVM infection*

219   As PVM-specific CD8$^+$ T-cells migrated relatively late to the lungs of PVM

220   infected mice, we wondered whether migration of other immune cells was delayed

221   also. Quantification of NK cells in the BAL demonstrated a prominent influx of NK

222   cells into the airways of PVM-infected mice at d. 6 of infection, when

223   approximately 50% of total infiltrating lymphocytes were NK cells (Fig. 2A, left

224   panel). In absolute numbers (Fig. 1A, right panel) NK cell responses in PVM-

225   infected mice peaked between days 8 and 10 of infection and then declined. In

226   comparison, in the airways of influenza strain HKx31-infected mice (Fig. 1A) a

227   large influx of NK cells, representing approximately 60% of total lymphocytes, was

228   detected already at d. 2 p.i. with absolute numbers of infiltrating NK cells peaking

229   at d. 3 of infection. Similar results were obtained in analyses of the BAL of hRSV-

230   infected mice (Supplemenary Fig. 1). Both in influenza- and in PVM-infected mice,

231   BAL NK cells displayed an activated phenotype (high CD69) and produced IFNγ

232   upon stimulation *ex vivo* (Fig. 2B, C), indicating that they were functional. Thus,

233   PVM-infected mice show a marked influx of NK cells into the airways, although at

234   a later time point than in mice infected with influenza or hRSV.

235   PVM is a natural mouse pathogen and, unlike in case of HKx31, only a few

236   viral particles suffice to establish severe disease in mice. To determine whether

237   the low numbers of infecting virus particles explains for the shifted kinetics of NK

238   cell responses in PVM compared to HKx31-infected mice, NK cell influx into the

239   airways of PVM-infected mice was compared to that in mice infected with the

240   mouse-adapted influenza strain PR8, which is more virulent than HKx31 and

241   therefore used at 100-1000 fold lower concentration. Still, like HKx31, infection

242   with PR8 (150 EID_{50}) induced a prominent early NK cell influx into the airways

243   (Fig. 2D, d. 2 and 4 p.i). Conversely, mice infected with a high dose of PVM (1250

244   pfu) lacked NK cells in the BAL at d. 2 p.i., and only minor numbers of NK cells

245   were detected at d. 4 p.i. (Fig. 2D). In conclusion, both CD8$^+$ T-cells and NK cells

246   migrate to the BAL at a much later time point following infection with PVM than

247   with influenza. The relatively late influx of NK cells into the airways of PVM-

248   infected mice is likely to be explained by specific properties of this pneumovirus

249   rather than by the low numbers of viral particles administered to cause infection.

250

251   *3.3. $P_{261-269}$-specific memory CD8$^+$ T-cells provide partial protection against PVM-*

252   *induced disease*

253   It has been shown that in PVM-infected mice, T-cells are responsible for

254   viral clearance, but are also involved in immunopathology [31]. To determine

255   whether PVM-specific memory CD8$^+$ T-cells may confer immune protection, mice

256   were immunized with GM-CSF-expanded BM-DC loaded with synthetic $P_{261-269}$

257   (DCp) and then challenged with PVM. As shown in Figs 3A and 3B, numbers of

258    $P_{261-269}$-specific CD8$^+$ T-cells detected in the BAL of immunized mice were

259   substantially higher than in non-immunized controls (Fig. 3A, B). Over the duration

260   of the infection, DCp-primed mice lost less weight (Fig. 3C), displayed significantly

261   reduced total-cell influx in the BAL (Fig. 3D), viral loads were significantly lower

262   than in non-immunized mice (Fig. 3E), and peribronchial and interstitial cellular

263   infiltrates were reduced (Supplementary Fig. 2), indicating an enhanced control of

264   disease and viral loads.

265   Since vaccination with FI-PVM elicits an enhanced Th2 response upon

266   PVM infection [40], we investigated the effect of DCp immunization on CD4 T-cell

267   differentiation during PVM challenge. Compared with FI-PVM-immunized controls,

268   mice immunized with $P_{261-269}$-loaded DC displayed elevated amounts of IFNγ

269   mRNA and cytokine levels in the lungs following challenge, indicating that they

270   had developed a Th1-skewed immune response (Fig. 4A, B; upper panels). In

271   contrast, FI-PVM immunized mice developed a Th2-skewed response, as

272   indicated by the relatively high levels of IL-4 in the lungs (Fig. 4A, B; lower panels)

273   and eosinophilia in two out of four mice (Fig. 4C, D). Thus, the presence of

274   memory CD8^{+} T-cells specific for a single PVM-epitope led to enhanced control of

275   virus replication and prevented Th2 skewing of PVM-induced CD4 T-cell

276   responses upon PVM challenge, leading to a reduction of PVM-induced disease.

277

278   *3.4. Protection conferred by adoptively transferred PVM-specific CD8^{+} T-cells*

279   Since immunization with $P_{261-269}$-loaded DC provided partial protection, we

280   decided to assess the protective capacity of the total PVM-specific CD8^{+} T-cell

281   response, targeting multiple epitopes. A mix of CD8^{+} T-cells enriched from the

282   spleen, MLN and lungs of PVM-infected or uninfected mice were adoptively

283   transferred into recipient mice that then were infected with PVM. At d. 7 p.i. a clear

284   population of $P_{261-269}$-tetramer^{+} cells was detectable in the lungs of mice that had

285   received CD8^{+} T-cells of PVM-infected donors, but not in the lungs of recipients

286   that had received naïve CD8^{+} T-cells of uninfected controls (Fig. 5A, B). In

287   addition, recipients receiving immune cells from infected mice showed significantly

288   reduced weight-loss and viral load (Fig. 5C, D). These results show that PVM-

289   specific CD8^{+} T-cells, despite being a major cause of pathology in pneumovirus

290   infections, can provide protection against PVM infection.

4. Discussion

Despite the fact that hRSV is a major cause of disease in infants, there still are major gaps in our knowledge of the host response against this virus. There is an increasing interest in using the natural mouse pathogen PVM to mimic and study severe pneumovirus infections. We have used this model to study the role of $CD8^+$ T-cells in conferring protection against disease. Influx of both NK and $CD8^+$ T-cells into the BAL of PVM-infected mice was markedly delayed compared to that in mice infected with influenza or hRSV (Fig. 1, 2). However, from d. 10 p.i. onwards, extremely high numbers of $CD8^+$ T-cells were present in the airways of PVM-infected mice, coinciding with disease. The relatively late immune activation seen in the PVM-infected mice was not explained by the quantities of administered viral particles, as both sublethal and lethal doses of PVM failed to induce an early NK cell influx in the infected respiratory tissue (Fig. 1), whereas both high dose HKx31 and low dose PR8 (representing comparable ID50s) caused an early NK cell influx, well detectable at d. 2 p.i. If not the quantities of administered particles, differing replication kinetics may explain the differences in kinetics of immune activation between PVM and influenza infection, although it should be noted that PVM rapidly replicates during the first days of infection, reaching titers of approximately 10^5 particles/lung at d.2 p.i. (Fig. 1) . Alternatively, the relatively late influx of lymphocytes into the airways of PVM-infected mice is consistent also with recent observations that the nonstructural proteins of PVM (NS1 and NS2) inhibit type I and type III interferon responses [27,28]. In these studies, inflammation in the airways of PVM-infected mice was found to be still limited at d. 3 p.i., while at d. 6 p.i., high levels of chemokines and cytokines such as MCP-1, RANTES, MIP-1α and IL-15 were produced [27,28]. These

316 chemokines are likely to attract NK cells to the airways, as well as CD8$^+$ T-cells

317 [31].

318   The finding that CD8$^+$ T-cells cause pathology in the PVM-mouse model

319 [31] has raised questions about the use of a vaccine designed to stimulate a

320 pneumovirus-specific CD8$^+$ T-cell response. However, we show that mice

321 immunized with BM-DCs pulsed with PVM P$_{261-269}$ displayed a Th1-skewed

322 immune response and reduced viral loads following challenge (Fig. 3 and 4),

323 suggesting that vaccine-induced CD8$^+$ T-cell memory protects against

324 pneumovirus-induced disease. In an earlier study [41], immunization with PVM

325 P$_{261-269}$ in IFA was unsuccessful in protecting mice against PVM-infection unless

326 co-administered with a PVM-derived CD4 T-cell epitope. Interestingly, the

327 peptide/IFA immunization protocol used in that study resulted in mixed Th1/Th2

328 responses to the included CD4 T-cell epitope, in contrast to the Th1 responses

329 observed in PVM-challenged DCp-immunized mice (Fig. 3). Thus, immunization-

330 induced PVM-specific memory CD8$^+$ T-cells protect against PVM-associated

331 disease, but the degree of protection and effects of immunization on CD4 T-cell

332 differentiation depend on the strategy for epitope delivery and used adjuvant.

333 Importantly, transfer of CD8$^+$ T-cells isolated from PVM-infected mice, which are

334 targeted to a broad range of epitopes, almost entirely abrogated weight-loss in

335 recipients and significantly reduced viral loads following challenge with PVM (Fig.

336 5). Taken together, the data presented here demonstrate that the presence of

337 already primed PVM-specific CD8$^+$ T-cells at the time point of PVM-infection leads

338 to enhanced control of viral loads and prevents T-cell-driven immunopathology.

339   In conclusion, we have shown PVM-specific CD8$^+$ T-cells provide partial

340 protection against PVM-induced disease, probably by preventing Th2 skewing of

341 PVM-specific immune responses and by early control of viral loads. Our findings

342　strongly suggest that pneumovirus vaccines designed to induce antigen-specific

343　CD8$^+$ T-cell memory may offer effective protection against pneumovirus-induced

344　disease.

345

349

350

351　**References**

352　[1] Easton AJ, Domachowske JB, Rosenberg HF. Animal pneumoviruses:

353　molecular genetics and pathogenesis. Clin Microbiol Rev 2004;17(2):390-412.

354　[2] Thompson WW, Shay DK, Weintraub E, Brammer L, Cox N, Anderson LJ et al.

355　Mortality associated with influenza and respiratory syncytial virus in the United

356　States. JAMA 2003;289(2):179-86.

357　[3] Chin J, Magoffin RL, Shearer LA, Schieble JH, Lennette EH. Field evaluation

358　of a respiratory syncytial virus vaccine and a trivalent parainfluenza virus vaccine

359　in a pediatric population. Am J Epidemiol 1969;89(4):449-63.

360　[4] Fulginiti VA, Eller JJ, Sieber OF, Joyner JW, Minamitani M, Meiklejohn G.

361　Respiratory virus immunization. I. A field trial of two inactivated respiratory virus

362　vaccines; an aqueous trivalent parainfluenza virus vaccine and an alum-

363　precipitated respiratory syncytial virus vaccine. Am J Epidemiol 1969;89(4):435-

364　48.

365   [5] Kapikian AZ, Mitchell RH, Chanock RM, Shvedoff RA, Stewart CE. An

366   epidemiologic study of altered clinical reactivity to respiratory syncytial (RS) virus

367   infection in children previously vaccinated with an inactivated RS virus vaccine.

368   Am J Epidemiol 1969;89(4):405-21.

369   [6] Kim HW, Canchola JG, Brandt CD, Pyles G, Chanock RM, Jensen K et al.

370   Respiratory syncytial virus disease in infants despite prior administration of

371   antigenic inactivated vaccine. Am J Epidemiol 1969;89(4):422-34.

372   [7] Hall CB, Walsh EE, Long CE, Schnabel KC. Immunity to and frequency of

373   reinfection with respiratory syncytial virus. J Infect Dis 1991;163(4):693-8.

374   [8] Piedra PA, Jewell AM, Cron SG, Atmar RL, Glezen WP. Correlates of immunity

375   to respiratory syncytial virus (RSV) associated-hospitalization: establishment of

376   minimum protective threshold levels of serum neutralizing antibodies. Vaccine

377   2003;21(24):3479-82.

378   [9] Falsey AR, Walsh EE. Relationship of serum antibody to risk of respiratory

379   syncytial virus infection in elderly adults. J Infect Dis 1998;177(2):463-6.

380   [10] Fenton C, Scott LJ, Plosker GL. Palivizumab: a review of its use as

381   prophylaxis for serious respiratory syncytial virus infection. Paediatr Drugs

382   2004;6(3):177-97.

383   [11] Henderson FW, Collier AM, Clyde WA,Jr, Denny FW. Respiratory-syncytial-

384   virus infections, reinfections and immunity. A prospective, longitudinal study in

385   young children. N Engl J Med 1979;300(10):530-4.

386   [12] Braciale TJ. Respiratory syncytial virus and T cells: interplay between the

387   virus and the host adaptive immune system. Proc Am Thorac Soc 2005;2(2):141-

388   6.

389   [13] Castilow EM, Olson MR, Varga SM. Understanding respiratory syncytial virus

390   (RSV) vaccine-enhanced disease. Immunol Res 2007;39(1-3):225-39.

391   [14] Ostler T, Ehl S. Pulmonary T cells induced by respiratory syncytial virus are

392   functional and can make an important contribution to long-lived protective

393   immunity. Eur J Immunol 2002;32(9):2562-9.

394   [15] Ostler T, Davidson W, Ehl S. Virus clearance and immunopathology by

395   CD8(+) T cells during infection with respiratory syncytial virus are mediated by

396   IFN-gamma. Eur J Immunol 2002;32(8):2117-23.

397   [16] Alwan WH, Record FM, Openshaw PJ. CD4+ T cells clear virus but augment

398   disease in mice infected with respiratory syncytial virus. Comparison with the

399   effects of CD8+ T cells. Clin Exp Immunol 1992;88(3):527-36.

400   [17] Cannon MJ, Openshaw PJ, Askonas BA. Cytotoxic T cells clear virus but

401   augment lung pathology in mice infected with respiratory syncytial virus. J Exp

402   Med 1988;168(3):1163-8.

403   [18] Graham BS, Bunton LA, Wright PF, Karzon DT. Role of T lymphocyte subsets

404   in the pathogenesis of primary infection and rechallenge with respiratory syncytial

405   virus in mice. J Clin Invest 1991;88(3):1026-33.

406 [19] Tregoning JS, Yamaguchi Y, Harker J, Wang B, Openshaw PJ. The role of T

407 cells in the enhancement of respiratory syncytial virus infection severity during

408 adult reinfection of neonatally sensitized mice. J Virol 2008;82(8):4115-24.

409 [20] Varga SM, Braciale TJ. RSV-induced immunopathology: dynamic interplay

410 between the virus and host immune response. Virology 2002;295(2):203-7.

411 [21] Hussell T, Baldwin CJ, O'Garra A, Openshaw PJ. CD8+ T cells control Th2-

412 driven pathology during pulmonary respiratory syncytial virus infection. Eur J

413 Immunol 1997;27(12):3341-9.

414 [22] Stevens WW, Sun J, Castillo JP, Braciale TJ. Pulmonary eosinophilia is

415 attenuated by early responding CD8(+) memory T cells in a murine model of RSV

416 vaccine-enhanced disease. Viral Immunol 2009;22(4):243-51.

417 [23] Srikiatkhachorn A, Braciale TJ. Virus-specific CD8+ T lymphocytes

418 downregulate T helper cell type 2 cytokine secretion and pulmonary eosinophilia

419 during experimental murine respiratory syncytial virus infection. J Exp Med

420 1997;186(3):421-32.

421 [24] Bossert B, Conzelmann KK. Respiratory syncytial virus (RSV) nonstructural

422 (NS) proteins as host range determinants: a chimeric bovine RSV with NS genes

423 from human RSV is attenuated in interferon-competent bovine cells. J Virol

424 2002;76(9):4287-93.

425 [25] Lo MS, Brazas RM, Holtzman MJ. Respiratory syncytial virus nonstructural

426 proteins NS1 and NS2 mediate inhibition of Stat2 expression and alpha/beta

427 interferon responsiveness. J Virol 2005;79(14):9315-9.

428 [26] Rosenberg HF, Bonville CA, Easton AJ, Domachowske JB. The pneumonia

429 virus of mice infection model for severe respiratory syncytial virus infection:

430 identifying novel targets for therapeutic intervention. Pharmacol Ther

431 2005;105(1):1-6.

432 [27] Buchholz UJ, Ward JM, Lamirande EW, Heinze B, Krempl CD, Collins PL.

433 Deletion of nonstructural proteins NS1 and NS2 from pneumonia virus of mice

434 attenuates viral replication and reduces pulmonary cytokine expression and

435 disease. J Virol 2009;83(4):1969-80.

436 [28] Heinze B, Frey S, Mordstein M, Schmitt-Graff A, Ehl S, Buchholz UJ et al.

437 Both Nonstructural Proteins NS1 and NS2 of Pneumonia Virus of Mice are

438 Inhibitors of the Interferon Type I and Type III Responses In Vivo. J Virol

439 2011;85(9):4071-84.

440 [29] Rosenberg HF, Domachowske JB. Pneumonia virus of mice: severe

441 respiratory infection in a natural host. Immunol Lett 2008;118(1):6-12.

442 [30] Claassen EA, van der Kant PA, Rychnavska ZS, van Bleek GM, Easton AJ,

443 van der Most RG. Activation and inactivation of antiviral CD8 T cell responses

444 during murine pneumovirus infection. J Immunol 2005;175(10):6597-604.

445 [31] Frey S, Krempl CD, Schmitt-Graff A, Ehl S. Role of T cells in virus control and

446 disease after infection with pneumonia virus of mice. J Virol 2008;82(23):11619-

447 27.

448 [32] Kruijsen D, Schijf MA, Lukens MV, van Uden NO, Kimpen JL, Coenjaerts FE

449 et al. Local innate and adaptive immune responses regulate inflammatory cell

450　influx into the lungs after vaccination with formalin inactivated RSV. Vaccine 2011;

451　29(15):2730-2741.

452　[33] Polakos NK, Klein I, Richter MV, Zaiss DM, Giannandrea M, Crispe IN et al.

453　Early intrahepatic accumulation of CD8+ T cells provides a source of effectors for

454　nonhepatic immune responses. J Immunol 2007;179(1):201-10.

455　[34] Zaiss DM, de Graaf N, Sijts AJ. The proteasome immunosubunit multicatalytic

456　endopeptidase complex-like 1 is a T-cell-intrinsic factor influencing homeostatic

457　expansion. Infect Immun 2008;76(3):1207-13.

458　[35] Garvey TL, Dyer KD, Ellis JA, Bonville CA, Foster B, Prussin C et al.

459　Inflammatory responses to pneumovirus infection in IFN-alpha beta R gene-

460　deleted mice. J Immunol 2005;175(7):4735-44.

461　[36] Chen W, Anton LC, Bennink JR, Yewdell JW. Dissecting the multifactorial

462　causes of immunodominance in class I-restricted T cell responses to viruses.

463　Immunity 2000;12(1):83-93.

464　[37] Chang J, Braciale TJ. Respiratory syncytial virus infection suppresses lung

465　CD8+ T-cell effector activity and peripheral CD8+ T-cell memory in the respiratory

466　tract. Nat Med 2002;8(1):54-60.

467　[38] Sherman LA, Burke TA, Biggs JA. Extracellular processing of peptide

468　antigens that bind class I major histocompatibility molecules. J Exp Med

469　1992;175(5):1221-6.

470　[39] Kulkarni AB, Morse HC,3rd, Bennink JR, Yewdell JW, Murphy BR.

471　Immunization of mice with vaccinia virus-M2 recombinant induces epitope-specific

472 and cross-reactive Kd-restricted CD8+ cytotoxic T cells. J Virol 1993;67(7):4086-

473 92.

474 [40] Percopo CM, Qiu Z, Phipps S, Foster PS, Domachowske JB, Rosenberg HF.

475 Pulmonary eosinophils and their role in immunopathologic responses to formalin-

476 inactivated pneumonia virus of mice. J Immunol 2009;183(1):604-12.

477 [41] Claassen EA, van Bleek GM, Rychnavska ZS, de Groot RJ, Hensen EJ,

478 Tijhaar EJ et al. Identification of a CD4 T cell epitope in the pneumonia virus of

479 mice glycoprotein and characterization of its role in protective immunity. Virology

480 2007;368(1):17-25.

481 [42] Stevens WW, Kim TS, Pujanauski LM, Hao X, Braciale TJ. Detection and

482 quantitation of eosinophils in the murine respiratory tract by flow cytometry. J

483 Immunol Methods 2007;327(1-2):63-74.

484

485

Figure Legends

Fig. 1. CD8$^+$ T-cell kinetics in PVM and influenza-infected mice. BALB/c mice

were infected *i.n.* with approximately 25 pfu PVM or 1×10^5 EID$_{50}$ influenza A/HK-

x31 and sacrificed at the indicated days p.i. (A) PVM virus titers in the right lung

determined by quantitative RT-PCR and converted to PVM-SH gene copy

numbers per lung. The dotted line indicates the detection limit. Results are shown

as mean $\pm$ SEM with 3 mice per group. (B) Frequency of total CD8$^+$ T-cells as

percentage of lymphocytes in the BAL determined by flow cytometry at the

indicated days p.i. Results are shown as mean $\pm$ SEM with 3 mice per group. (C)

Frequencies of virus-specific CD8$^+$ T-cells in the BAL were determined by staining

with MHC class I tetramers loaded with NP$_{147-155}$ (influenza tetramer) or M2$_{82-290}$

(hRSV tetramer), and tetramers loaded with unrelated peptides were used to

measure background staining. The percentage of virus-specific CD8$^+$ T-cells in the

BAL of influenza (left graph) or hRSV (right graph) infected mice (CD62L$^-$

tetramer+) are shown after subtraction of background staining. (D, E) Frequencies

of virus-specific CD8$^+$ T-cells in the BAL of PVM infected mice, determined as

described in (C) with P$_{261-269}$-peptide loaded MHC class I tetramers. (D) Graph

showing the results of individual mice and (E) representative FACS plots (gated

on CD8$^+$ cells) show the percentage of PVM tetramer+ (tet$^+$) or hRSV tetramer$^+$

CD62L$^-$ cells at the indicated days p.i. (F, G) BAL cells from PVM-infected mice

were restimulated *ex vivo* for 6h in the presence of monensin with or without P$_{261-}$

$_{269}$ peptide. (F) Corresponding graphs showing the results of individual mice

(background frequencies in the absence of peptide are subtracted) and (G),

representative FACS plots showing frequencies of IFNγ^+ CD8$^+$ cells after peptide

510 restimulation. Data are representative of two independent experiments. BAL of

511 uninfected mice did not contain any cells or detectable viral loads.

512

513

514 **Fig. 2.** NK cell responses in PVM- compared to influenza-infected mice. BALB/c

515 mice were infected *i.n.* with approximately 25 pfu PVM or 1×10^5 EID_{50} influenza

516 A/HK-x31 and sacrificed at the indicated days p.i. (A) NK cells ($TCR\beta^-DX5^+$) as

517 percentage of total lymphocytes (left panel) or in absolute numbers (right panel) in

518 the BAL, as determined by flowcytometry. (B) Mean fluorescence intensities (MFI)

519 of CD69 expression on NK cells in the BAL. (C) Percentage of IFNγ producing NK

520 cells in the BAL after *ex vivo* restimulation with YAC cells (1:1) in the presence of

521 monensin for 6h. (D) Mice were infected with 150 EID_{50} influenza PR8, 25 pfu

522 PVM (normal dose) or 1250 pfu PVM (high dose) and absolute numbers of NK

523 cells ($DX5^+NKp46^+TCR\beta^-$) in the BAL were determined. Results are shown as

524 mean ± SEM for 3 mice per group. n.d., not determined.

525

526

527 **Fig. 3.** Effects of DCp immunization on control of PVM infection. Mice were

528 immunized *i.v.* with 5×10^6 $P_{261-269}$-loaded BM-DCs or left untreated, and infected

529 *i.n.* with approximately 15 pfu PVM 3-5 weeks later. 4-5 mice per group were

530 sacrificed on d. 8 and 14 after PVM infection. (A, B) Frequency of $P_{261-269}$-specific

531 $CD8^+$ cells in the BAL at d. 14 p.i. determined by tetramer staining as described in

532 the legend to Fig. 2. (A) Representative FACS plots (gated on $CD8^+$ cells), and (B)

533 corresponding graphs showing results for individual mice. (C) Body weight of

534 individual mice as a percentage of their initial weight. (D) Total numbers of cells in

535 the BAL at d. 8 p.i. (E) Virus titer in the right lung determined by quantitative RT-

536 PCR and converted to PVM-SH gene copy numbers. Data are representative of

537 two independent experiments. Statistical analysis was performed using a Mann-

538 Whitney U-test. *, p<0.05

539

540

541 **Fig. 4.** Cytokine production and eosinophils in the airways of PVM-infected, DCp-

542 compared to FI-PVM-immunized mice. 4-5 mice per group were immunized *i.v.*

543 with 5 x 10^6 $P_{261-269}$-loaded BM-DCs, or *s.c.* with FI-PVM, and infected *i.n.* with

544 approximately 15 pfu PVM 3-5 weeks later. (A) Relative expression of IFNγ (upper

545 graph) or IL-4 (lower graph) mRNA in the lungs 5 days after PVM infection,

546 determined by Q RT-PCR. (B) Levels of IFNγ (upper graph)and IL-4 (lower graph)

547 in the BAL fluid on d. 5 p.i., determined by luminex. (C) FACS plots showing an

548 example of CD11c and Siglec-F staining on BAL cells of immunized mice 14 days

549 after PVM infection. Gated samples were eosinophils (CD11c$^-$Siglec-F$^+$) as

550 described [42]. (D) Frequency of eosinophils in the BAL of individual immunized

551 mice 14 days after PVM infection, determined by flow cytometry. Statistical

552 analysis was performed using a Mann-Whitney U-test. *, p<0.05

553

554

555 **Fig. 5.** Effects of CD8$^+$ T-cell transfer on PVM infection. CD8$^+$ T-cells enriched

556 from pooled lung-, spleen- and MLN-cells of PVM-infected (d. 14 p.i.) or naïve

557 donor mice were transferred *i.v.* into recipient mice that were subsequently

558 infected with approximately 25 pfu PVM and sacrificed at d. 7 p.i. (A)

559 Representative FACS plots of gated CD8$^+$ cells showing $P_{261-269}$-specific T cells

560 (CD62L$^-$PVM tet$^+$) in the lungs of mice that received CD8$^+$ T-cells of PVM-infected

561 (right) or naïve (left) donors. (B) Frequencies of $P_{261-269}$-specific CD8$^+$ cells in the

562   lungs, determined by tetramer staining. (C) Body weight of individual mice as

563   percentage of their initial weight at the indicated days p.i. (D) Virus titer in the right

564   lung determined by Q RT-PCR and converted to PVM-SH copy numbers.

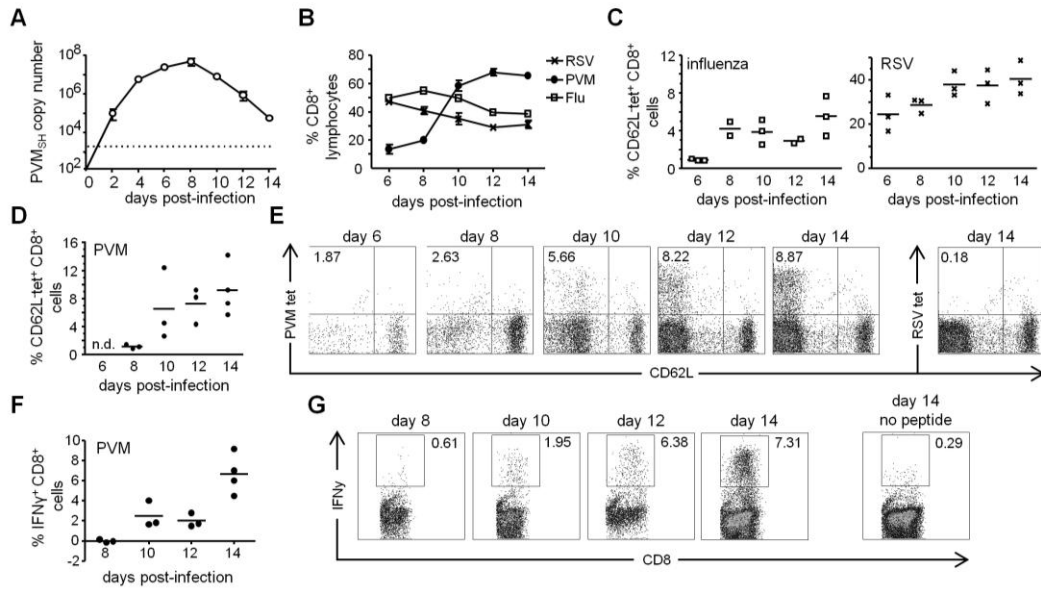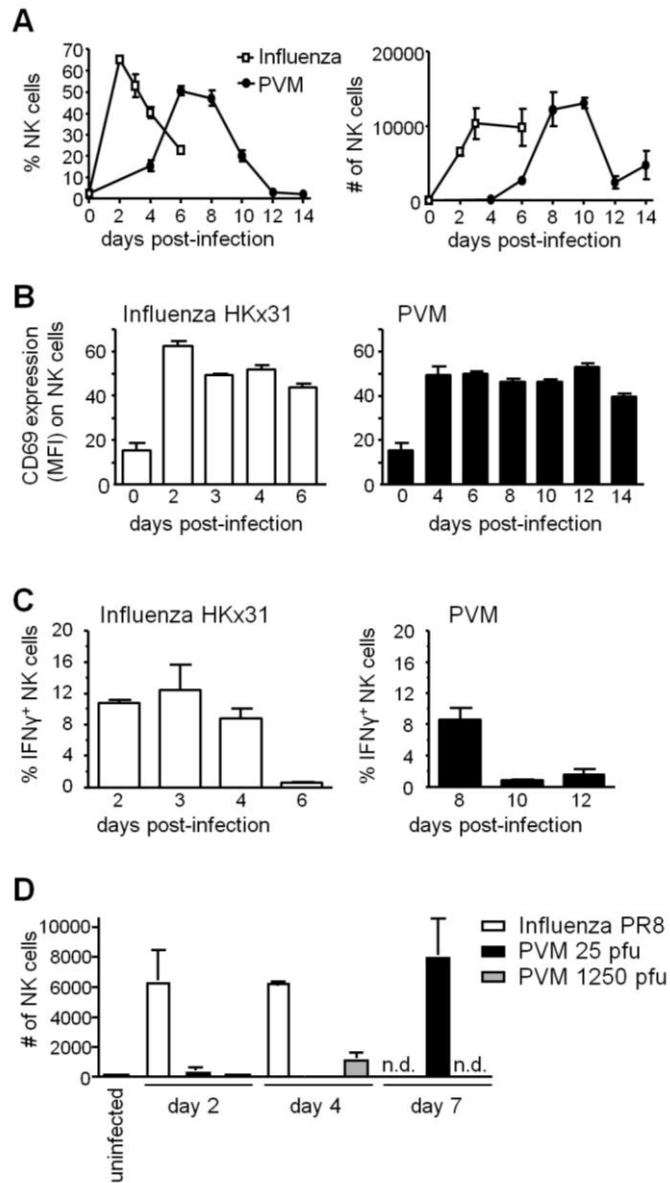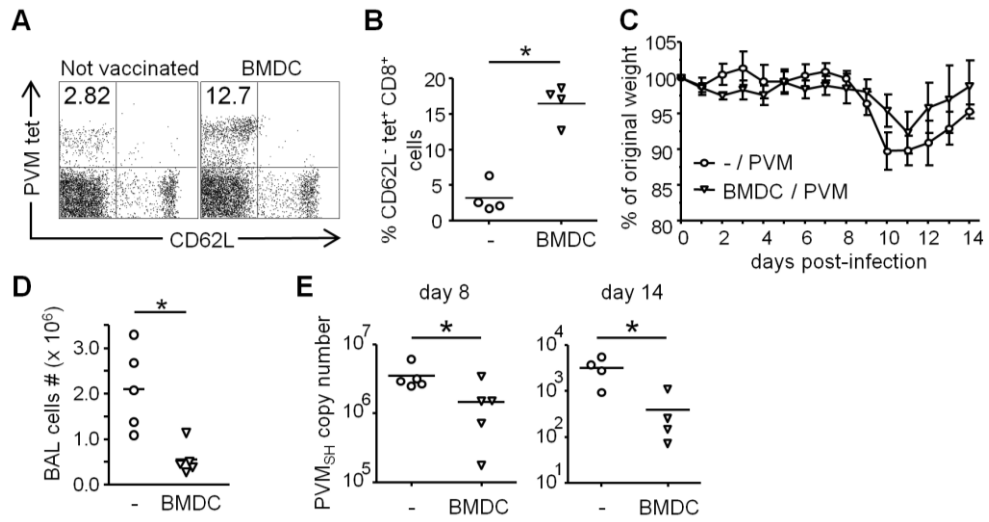565   Statistical analysis was performed using a Mann-Whitney U-test. *, p<0.05

566
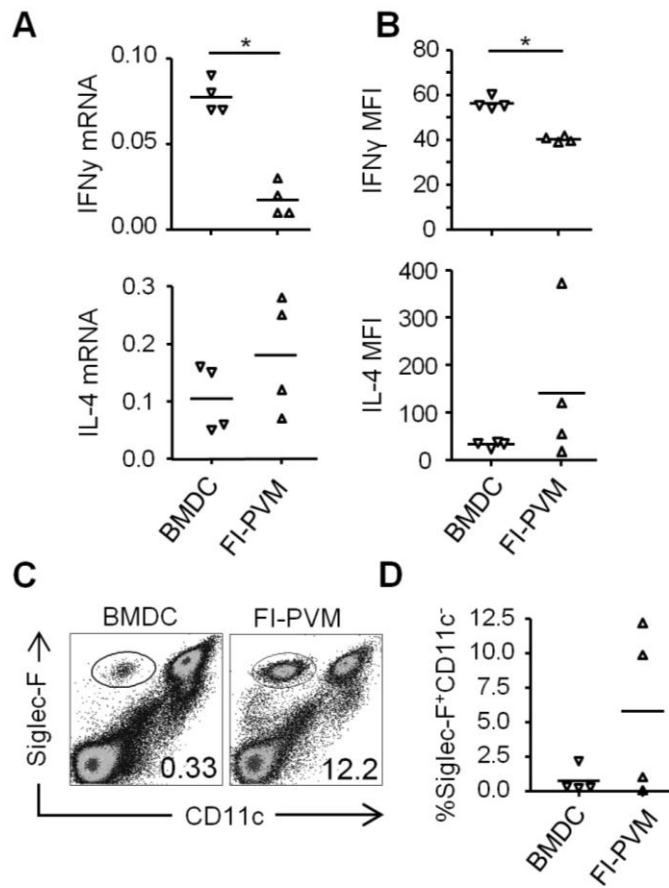
Figure 1

Figure 2

Figure 3

Figure 4

A

IFNγ mRNA

IL-4 mRNA

B

IFNγ MFI

IL-4 MFI

BMDC   FI-PVM

C

Siglec-F →

BMDC   FI-PVM

0.33   12.2

CD11c →

D

%Siglec-F⁺CD11c⁻

BMDC   FI-PVM

Figure 5